Overtopping of Coastal Structures by Tsunami Waves

Miguel Esteban [1,*]**, Toni Glasbergen** [2]**, Tomoyuki Takabatake** [3]**, Bas Hofland** [2]**,**
Shinsaku Nishizaki [3]**, Yuta Nishida** [3]**, Jacob Stolle** [4] **, Ioan Nistor** [4]**, Jeremy Bricker** [2]**,**
Hiroshi Takagi [5] **and Tomoya Shibayama** [3]

[1]   Graduate School of Frontier Sciences, The University of Tokyo, 5-1-5 Kashiwanoha, Chiba 277-8563, Japan
[2]   Department of Civil Engineering and Geosciences, Delft University of Technology, Stevinweg 1,
     P.O. Box 5048, Delft 2600GA, The Netherlands; toniglasbergen92@gmail.com (T.G.);
     b.hofland@tudelft.nl (B.H.); J.D.Bricker@tudelft.nl (J.B.)
[3]   Department of Civil and Environmental Engineering, Waseda University, 3-4-1 Ookubo, Tokyo 169-8555,
     Japan; tomoyuki.taka.8821@gmail.com (T.T.); shinsaku-nisshi@fuji.waseda.jp (S.N.);
     yuta325@ruri.waseda.jp (Y.N.); shibayama@waseda.jp (T.S.)
[4]   Department of Civil Engineering, University of Ottawa, 161 Louis Pasteur, Ottawa, ON CBY A306, Canada;
     jstol065@uottawa.ca (J.S.); inistor@uottawa.ca (I.N.)
[5]   Tokyo Institute of Technology, Tokyo 152-8550, Japan; takagi@ide.titech.ac.jp
*   Correspondence: esteban.fagan@gmail.com; Tel.: +81-80-4026-7791

Abstract: Following the *2011 Tohoku Earthquake and Tsunami*, Japanese tsunami protection guidelines stipulate that coastal defences should ensure that settlements are shielded from the coastal inundation that would result from Level 1 tsunami events (with return periods in the order of about 100 years). However, the overtopping mechanism and leeward inundation heights of tsunami bores as they hit coastal structures has received little attention in the past. To ascertain this phenomenon, the authors conducted physical experiments using a dam-break mechanism, which could generate bores that overtopped different types of structures. The results indicate that it is necessary to move away from only considering the tsunami inundation height at the beach, and also consider the bore velocity as it approaches the onshore area. The authors also prepared a simple, conservative method of estimating the inundation height after a structure of a given height, provided that the incident bore velocity and height are known.

Keywords: coastal dyke; dam break; tsunami; overtopping; evacuation

1. Introduction

The *2011 Tohoku Earthquake and Tsunami* (herein referred to as "the event") devastated much of the northeast coast of Japan, and is considered to be one of the most severe events to have affected Japan since historical records began. In the weeks that followed the event, the *2011 Tohoku Earthquake Tsunami* Joint Survey Group's measured the maximum tsunami inundation and run-up heights with values of between 10 and 40 m along the Tohoku coastline [1]. As a result, many people lost their lives, and reports issued by the Japanese National Police Agency mention 15,894 confirmed deaths and 2561 people still missing [2]. Furthermore, the Japanese Cabinet Office (2011) stated that 169 billion US$ worth of assets were lost, which is equivalent to approximately 3% of the country's GDP [3]. Consequently, in the years that followed, the reliability of tsunami protection structures is being re-assessed.

The 2011 event is currently considered a Level 2 tsunami, as it is believed to have a return period greater than 1 in 1000 years [4]. Essentially, following the *2011 Tohoku Earthquake and Tsunami*, the Japanese coastal engineering community has classified tsunami events into two different levels, according to their level of severity and intensity [4]. Level 1 events correspond to a return period

of several decades to 100+ years and would result in inundation levels typically around 7 to 10 m. Level 2 events would be less frequent, occurring every few hundred to a few thousand years, and the inundation heights would be much larger, over 10 m. The risk management strategy that should be implement would depend on the type of tsunami level and countermeasure that are considered. "Hard measures", such as breakwaters or coastal protection dykes, should be strong enough to protect against the loss of life and property for a Level 1 event. However, it is accepted that such coastal dykes would be overtopped by Level 2 events, and that coastal residents would have rely on "soft measures", such as evacuation procedures and tsunami shelters. Nevertheless, hard measures would also have a secondary role to play in delaying the incoming wave and giving residents more time to evacuate [5]. This means that the dykes should not collapse while being overtopped during a level 2 tsunami.

A number of different field surveys reports have highlighted a variety of failure mechanisms of coastal structures [2,6–8]. Most of these structures were not strong enough in terms of structural stability and hydraulic performance, and often failed catastrophically as they were overtopped by tsunami waves or tsunami-induced inundation [2,8]. Prior to the 2011 event, a number of laboratory experiments had been performed regarding how to design dykes and vertical structures against wind waves [9,10], including assessments of the reliability of these structures [11]. Tanimoto et al. [12] performed large-scale experiments using solitary waves on a vertical breakwater, which resulted in the development of a formula for calculating wave pressure. Ikeno et al. [13,14] used bore-type tsunami waves, and modified Tanimoto's formula by introducing an additional coefficient to account for wave breaking. Mizutani and Imamura [15] conducted model experiments with a bore overflowing a dike on a horizontal bed, which they then used to propose a set of formulae to calculate the maximum wave pressure behind the dike. Esteban et al. [16] calculated the deformation of the rubble mound foundation of a caisson breakwater against a variety of types of solitary waves and bore-like conditions. Esteban et al. [17,18] proposed formulas for the design of caisson breakwaters and armour against tsunami waves. However, the use of solitary waves in tsunami modelling has been challenged due to the relatively short distance between the source region and coast when compared to the distance in which a soliton forms [19]. As such, the use of solitary waves can only consider the incipient motion of the tsunami wave [20]. Other researchers [6,21,22] proposed methods to design the armour of breakwaters against tsunami attack, focusing on the current velocity and the overtopping effect, though the parameters that are used in these studies are not easy to estimate.

Based on these laboratory experiments and post-tsunami field investigations [6,21,22], it is evident that beach bathymetry, onshore coastal topography, coastal geomorphology, coastal structure geometry, and (tsunami) wave conditions, all influence the failure modes and mechanisms of coastal structures [8]. Particularly, for the case of dykes a number of authors [6,8,23] identified how leeward toe scour was the leading failure mechanism, though a number of other distinct mechanisms were also highlighted [6,8].

Computer simulations have shown how, despite failing, these types of structures can be effective in mitigating tsunami damage [24–26]. Field surveys corroborate such numerical modelling. For instance, the ASCE-EERI examined areas inside and outside sea-walls and found a significant difference between them, with damage being far more significant outside of the walls [27]. These results are corroborated by other authors [28], which indicate that even when overtopped, coastal defences can help to mitigate tsunami effects [29]. In the case of offshore breakwaters, the fatality ratio of ports that are equipped with breakwaters was smaller than in the case of ports without breakwaters [30]. Immediately after the 2011 Tohoku disaster, a Japanese governmental research institute publicized their analysis of how the tsunami height behind the Kamaishi Tsunami breakwater was likely reduced from 13.7 m to 8.0 m, and the presence of the tsunami breakwater also gave residents an extra 6 min to evacuate. However, this estimation may not be completely reliable, as it neglected the influence of a number of breakwater sections that were knocked off during the tsunami [31]. Normal breakwaters were basically designed to reflect wind waves, and thus in general the reduction of the tsunami impact due to these structures should also not be overestimated [32].

However, despite all of the research that was conducted on the structural behavior of structures under tsunami attack, to the authors' knowledge, comparatively little experimental work has been carried out on the overtopping nature of the tsunami-induced flows over a dyke. Understanding this phenomenon is of critical importance in order to design such structures. The adequate design of coastal dykes can provide extra time for local residents to evacuate, without the need to construct them high enough that they would become economically unfeasible [33]. Several researchers have studied evacuation in specific locations, such as Kamakura City (Japan), highlighting the importance of evacuation procedures and communication to improve human evacuation in the case of a disaster [34,35]. However, the presence of higher dykes has been shown to be able to provide more time for residents to evacuate [33]. To properly understand the benefits of a coastal dyke, determining the volume of water, velocity (*v*), and flooding depth (*d*) that can result from an overtopping tsunami is critical. Generally, *dv* values that are higher than 0.5 m^2/s can result in 50% mortality, increasing to almost 100% when $dv > 2$ m^2/s [36].

Thus, in the present work, the authors investigated the overtopping flow patterns that result from a variety of different incident bore-type tsunami conditions. Laboratory experiments were carried out using a dam-break generation mechanism, with a bathymetry that simulates a typical beach profile along the Japanese coast, protected by various types of structures. In doing so, the authors hypothesized that the energy of the bore as it approached the structure will determine whether it will be overtopped or not. Essentially, lower velocity bores that have incident wave heights that are lower than the height of the structure would be stopped, with higher velocity bores overtopping the dykes.

Additionally, the authors attempted to provide some general design guidelines regarding how high a structure would have to be to protect against a tsunami, which would obviously be highly dependent on its location. Those facing a direct tsunami attack (characterized by high velocity waves that would otherwise result in a high run-up) would require to be built to a higher level than those that are located in a more sheltered location (which might face a "rapidly rising tide" or slow bore, that would result in lower run-up).

2. Experimental Program

Laboratory experiments using a dam break generation mechanism were performed in a wave flume (dimensions 14 m × 0.41 m × 0.6 m) at Waseda University, Tokyo, Japan. Froude scaling of 1:50 was used. A schematic representation of the wave tank and gate used to generate the dam break wave is shown in Figure 1. On one side of the tank, a dam break generation mechanism was constructed. Its rapidly opening gate was operated by a system of pulleys that were attached to a heavy weight. The release of the weight lifted the gate, and, as this weight was kept constant, the speed at which the gate was raised was similar for all of the experiments. The reservoir was 4.5 m long in order to ensure that a long bore was generated (given the dimensions of the tank and the water level behind the gate, between 18.9 and 37.8 m^3 of water were released in every experiment).

The "wave half-period", $T/2$, was estimated from the wave profile in the cases where no structure was present. For the cases when the amount of water in the tank was limited, this value could be calculated precisely ($T/2 = 10.6$ s for $h = 30$ cm and $d = 0$ cm, for example), though as the amount of the water behind the reservoir increased the reflected wave arrived at the wave gauge before a complete wave cycle could be estimated (hence, it is only possible to conclude that $T/2 > 16.1$ for $h = 60$ cm and $d = 0$ cm). Nevertheless, having $T/2 > 10$ s essentially allowed for the overtopping experiment to reach a quasi-stationary overtopping flow, similar to that observed during video footage of the 2011 Tohoku event. A total matrix of 12 experimental conditions were carried out, for $d = 30$, 40, 50, and 60 cm, and $h = 0$, 10 and 20 cm.

A metal false bed was placed in front of the gate, with the beginning of the sloping section starting 5 cm from the edge of the gate. The false bed was situated 20 cm above the horizontal flume bed, and the sloping section was 2 m long, resulting in a slope of 1:10. The main testing section was located at the other side of the tank, 1.65 m away from the edge of the sloping section. In this area, three different

coastal structures were tested: (1) a coastal dyke, (2) a low tsunami wall (15 cm high), and (3) a high tsunami wall (39 cm high, to attempt to reproduce the effect of a wall of "infinite height"). The high tsunami wall was made using an acrylic panel (Figure 2). The low tsunami wall was constructed using a concrete block 15 cm high and 10 cm wide (Figure 2). The dyke was made using a combination of acrylic panels and a hollow metallic structure, (9.5 cm high, 26 cm long across the base and 6 cm wide at the top), which is typical of the types of dykes that can be seen along the Japanese coastline (Figure 2). All of the structures were fixed to the sides of the tank using silicon and were completely sealed, with no movement being observed in any of the structures during the experiments. Behind the structure, a wave absorption beach was constructed, under which there was a drain to remove all of the excess water after each experiment.

A number of wave gauges (WG) and velocity meters (VM) were placed throughout the tank to measure the wave transformation and the incident wave conditions, as shown in Figure 1. Table 1 shows a summary of the instrumentation positions that were used. The velocity meters were placed at the top of the structure and 15 cm behind it, to measure the overtopping conditions. The experiments were also repeated without any structures present in the tank, in order to evaluate the hydrodynamic conditions of the wave, particularly focusing on the velocity profile just before the structure. The velocity meters (KENEK VMT2-200-04P, 04PL. Kenek, Tokyo, Japan) that were used in the experiment were electromagnetic current meters (ECMs). The maximum range of measurement was 200 cm/s, and a low pass filter of 20 Hz was applied after the data acquisition. Due to cavitation around the probe head and air bubbles entrained within the turbulent bore, the complete velocity profile could not be captured for the entire length of the experiments. Thus, the authors regarded the measurements as approximate reference values, and the bore front velocities were calculated from more reliable measured data obtained from the wave gauges (WGs), as discussed later. The instruments were connected to a data logging system (KENEK ADS2016. Kenek, Tokyo, Japan), which was itself connected to a PC. The sampling frequency of all the measurements was 200 Hz. A Nikon D5200 camera (Nikon, Tokyo, Japan) was mounted on a tripod, directly in front of the structures, to observe the profile of the bores as they impacted the structures, and their corresponding overflow patterns.

At the beginning of each experiment, the tank was drained and filled to a specified height with water (both for the water in the reservoir and in front of the gate). Wet bed conditions were used for all of the experiments, as the false bed was not dried between tests. To ensure replicability, certain experimental conditions were repeated several times, as will be explained later.
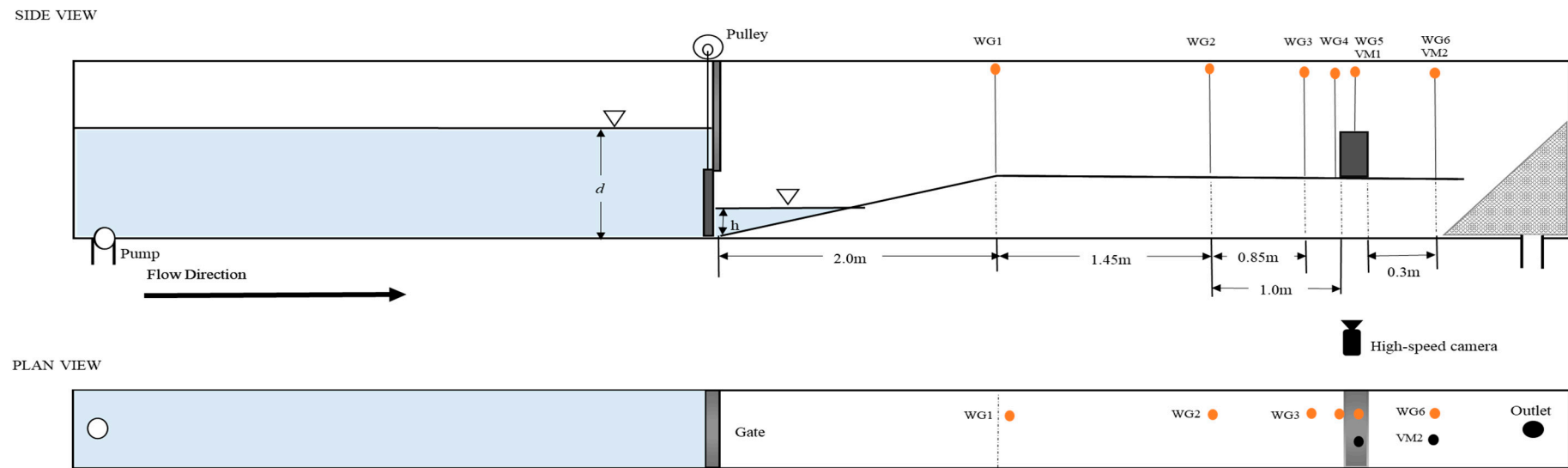
SIDE VIEW

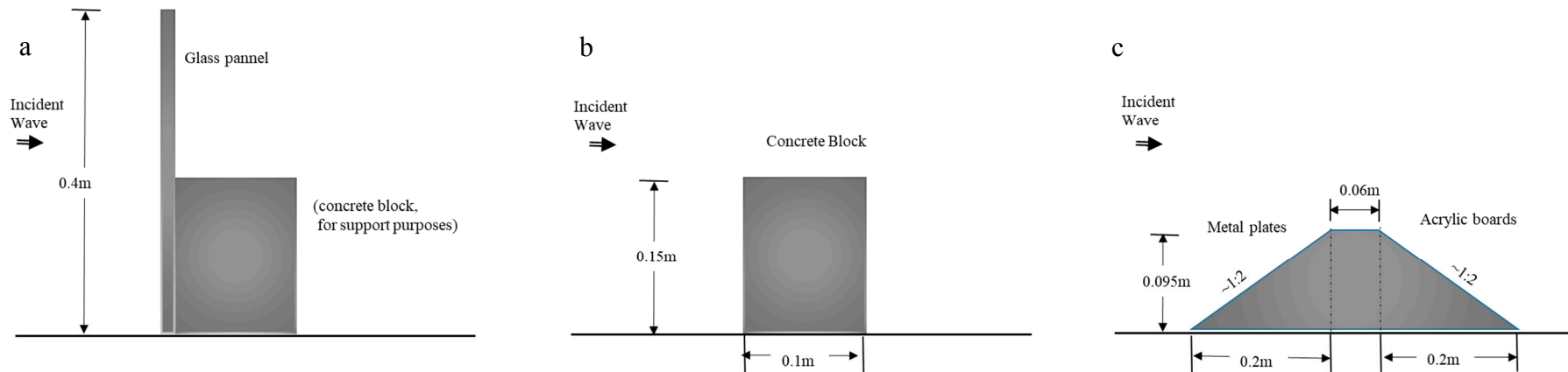**Figure 1.** Schematic of the wave flume and intrumentation (not to scale).

Figure 2. Schematic and photographs of the structure types tested (not to scale). From left to right, (**a**) "high vertical wall", (**b**) "low vertical wall" and (**c**) dyke.

Table 1. Summary of experimental conditions and testing (the table will be referred to throughout the results section, and some definitions appear in diagrams within that section).

Structure Type		No Structure		High Vertical Wall (Non-Overtopped)		Low Vertical Wall			Dyke		
		H_i (cm)	V_i (m/s)	H_{f0} (cm)		H_f (cm)	H_o (cm)	H_b (cm)	H_f (cm)	H_o (cm)	H_b (cm)
d (cm)	h (cm)	WG5	WG2-4	WG3	WG4	WG3	WG5	WG6	WG3	WG5	WG6
30	0	3.42	1.24	8.24	6.8	8.57	0	0	8.06	0.41	1.43
	10	3.67	1.15	7.79	6.81	7.15	0	0.02	8.57	0	0.61
	20	3.73	0.88	8.2	6.52	7.49	0	0.02	8.7	0.04	0.12
40	0	5.49	1.68	16.15	13.1	15.21	0.9	1.48	13.73	5.55	4
	10	5.64	1.37	14.59	11.7	14.46	0.21	1.41	13.39	4.41	2.4
	20	5.64	1.79	15.41	12.9	14.85	0.57	1.62	13.58	3.89	2.58
50	0	8.59	2.12	24.3	20.6	*21.04*	*10.76*	*5.31*	*17.61*	*11.35*	*7.56*
	10	7.79	1.92	22.38	18.2	19.28	4.92	3.26	17.11	9.22	6.88
	20	8.32	1.66	21.41	19.7	20.16	5.31	4.3	17.97	10.45	7.38
60	0	12.17	2.59	33.69	>30	27.55	16.33	9.45	20.32	16	9.92
	10	10.74	2.43	28.61	>30	24.35	11.11	6.95	20.36	13.16	8.95
	20	10.27	2.7	28.63	24.2	24.17	12.38	6.88	20.89	13.48	10.12

Note: Numbers in bold italics shows the experimental conditions ($d = 50$, $h = 10$ cm, for both the low vertical wall and the dyke) that were repeated 5 times.

3. Results

3.1. Experiment Repeatability

To test whether the experiments were consistent and reproducible between tests, the "low tsunami wall" and "dyke" structure experiments with $d = 50$ cm and $h = 0$ cm were repeated five times (Table 1). The wave heights and velocities at each of the wave gauges and velocity metres for the low tsunami wall are plotted in Figure 3. This figure shows that the standard deviation of the profile of the wave surface at each gauge was low, with a maximum error of 11.41% and 8.47% for WG5 and WG6, respectively (WG1 and WG3 showed errors of less than 2%). However, the velocity measurements were less consistent. For VM1, there was an error of 6.21%, though this climbed to 67.15% for the case of VM2. The errors for the dyke experiments were similar for the case of WG1 and WG3, and slightly lower for WG5 and WG6 (under 6.5%), and the velocity metres (9.99% and 45.14% for VM1 and VM2, respectively). The VM is an electromagnetic instrument, and does not produce good results when the void ratio is high (i.e., when there is much air entrainment), possibly indicating why VM1 was more stable than VM2. Thus, although the overtopping pattern and depth after the structure is consistent, the velocity profile results need to be treated with caution.
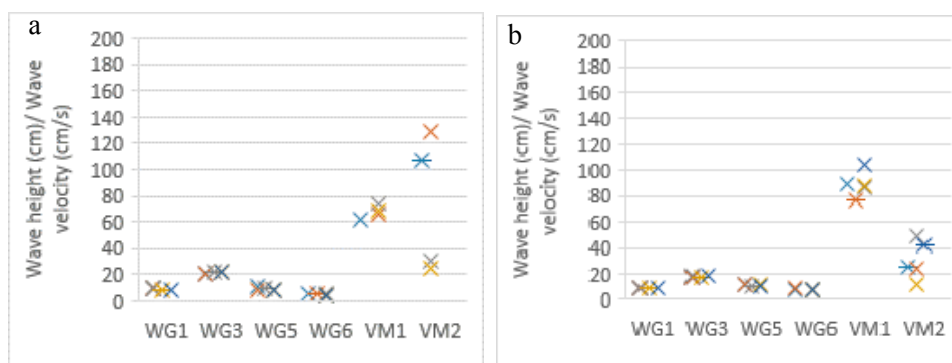

Figure 3. Values for wave height (for the case of the wave gauges, WG) and wave velocity for the velocity metres (VM) for the "low tsunami wall" (**a**) and "dyke" (**b**) experiments with ($d = 50$ cm and $h = 0$ cm).The results of all five repetition of of the same test are plotted, showing how for wave gauges the consistency is high, though there is much scattering of values for the velocity metres.

3.2. Dam Break Wave Profile

For some of the experiments, the velocity of the incident bores exceeded the capabilities of the velocity metres (200 cm/s). In addition, as the ratio of the velocities to the inundation depths at the measurement points was large, some air pockets were trapped behind the probes, resulting in missing data points. To overcome this problem, the bore front velocity was used to approximate the maximum kinetic energy of the wave. Dressler [37] analytically showed through the Saint-Venant equations that the flow velocity at a single point would decay from the bore front velocity over time. The analytical solution was validated through dam-break experiments over various bed surfaces [36,38]. Chanson [39] estimated that the flow velocity in the turbulent bore tip was approximately equal to the bore front velocity. The present experiments were conducted over a flat, unobstructed, horizontal surface, and thus the bore front velocity would represent the maximum velocity of the flow.

The bore front velocity was calculated by computing the time for the bore tip to travel between WG2 and WG4—situated exactly 1.0 m apart—for the case when no structure was present in the tank, as shown in Figure 4. The incident wave height (H_i) was taken as the maximum height of the wave as it traversed WG5, as this wave gauge was placed at the centre of the location where the structures would later be placed. The calculated values for V_i and H_i are shown in Table 1. When no structure was installed, the wave profile appeared uniform as it traversed the tank (Figure 4), and did not undergo any significant changes in profile (i.e., there was no change in wave profile between WG4 and WG5, which was obviously not the case once the structures were placed, see Figure 5).
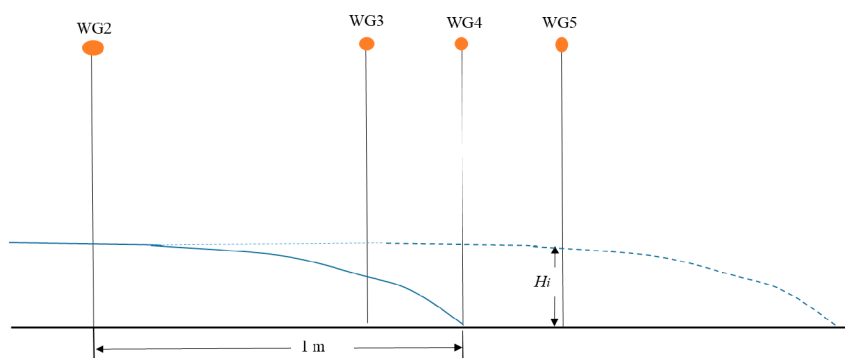

Figure 4. Calculation of the bore velocity V_i. The continous line represents the wave profile when the bore reaches WG4. The incident wave height H_i was taken as the maximum water lever at the position of WG5 (discontinous line shows the wave profile at this point).
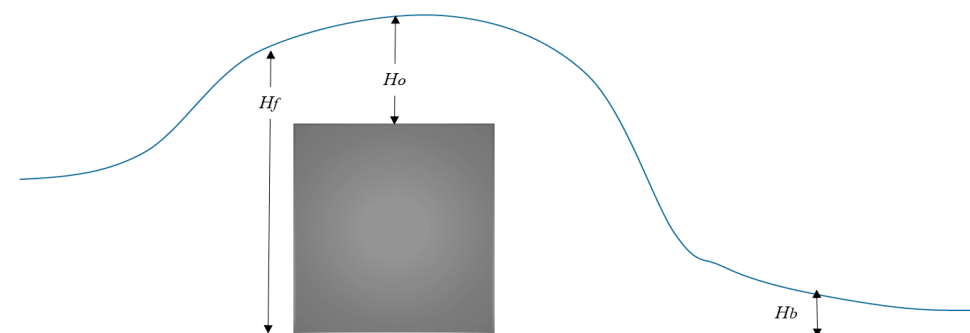

Figure 5. Wave parameters. H_f, H_o, and H_b are the maximum values of the surface profile of the wave as it impacts, overtops and continues to run behind the structure, given by WG3, WG5, and WG6, respectively.

When the structures were placed in the tank, the incident bore impacted the structure, and eventually overtopped it if there was sufficient energy in it. To analyse the overtopping effect, a

number of parameters were defined, as shown in Figure 5. H_f, H_o, and H_b are the maximum values of the water surface elevation of the bore as it impacts, overtops, and continues to run behind the structure, given by WG3, WG5, and WG6, respectively. The time history of water elevation for each of these wave gauges is given in Figure 6, for the case of the low tsunami wall, $h = 0$ cm and $d = 30, 40, 50$, and 60 cm. From Figure 5 it is clear that as the initial depth of the water behind the gate increased, the kinetic energy in the bore also increased, resulting in a greater H_o and H_b. Figure 7 shows the corresponding photograph frames for each of the cases shown in Figure 6, and also includes the overtopping profiles of the dykes.

Figure 8 shows a photographic comparison of the incident and overtopping wave profiles of the three structures studied, for $d = 50$ cm and $h = 0$ cm. In all of the cases the bore rapidly approached the structure and, after impacting, began to overtop it if there was enough energy in the bore. A quasi-stationary overtopping flow was achieved, which would last several minutes in real life tsunamis, though in the experiment it only lasted a few seconds (as eventually the water in the tank runs out).

3.3. Inundation Height after the Structure

According to basic wave hydraulics, the energy of the incoming wave as it traverses WG5 for the case when no structure is present would theoretically be given by the expression:

$$E_i = \frac{H_i^2}{2g} + H_i \tag{1}$$

where E_i is the specific energy head, V_i is the maximum incident bore front velocity in front of the structure, g is the acceleration due to gravity, and H_i is the maximum incident bore wave depth, as defined in Figures 4 and 5. It should be noted that the authors calculated the specific energy using slightly different times and locations of V_i and H_i, while acknowledging that it is formally necessary to use the V_i and H_i recorded at the same time. Still, the bore front gives a first estimate of the maximum particle velocity, and the velocity is not expected to change between the point of measurement and the location of the structure.

The authors first summarized the data of the high wall case, using the maximum value (defined as H_{ff}) recorded at WG4, placed close to the front of the high seawall. In this case, as the tsunami did not overtop the seawall, H_{ff} can be regarded as the maximum run up height in front of the structure (Figure 9). Figure 10 shows the relationship between H_{ff} and H_i, $V_i/2g$ (velocity head), and E_i, respectively (except the results of $d = 60$, $h = 0$ and $d = 60$, $h = 10$, as H_{ff} exceeded the capability of WG4 (30 cm) in these cases). It can be seen from Figure 10a that H_{ff} is higher than H_i in all of the cases (all results are plotted above the black line). This means that it is possible for the tsunami to overtop the structure even if the tsunami height is lower than it, indicating the difficulty and limitations when deciding an appropriate seawall height using only the incident tsunami height as a parameter. When a wall of sufficient height is present and the tsunami can be completely stopped, all of the energy (sum of the potential and kinetic energy) of the incident bore will have been transformed into the potential energy in front of the seawall (if the energy loss that takes place when the tsunami attacks the seawall is neglected). Thus, even if the potential energy of the tsunami (essentially, the bore height) is low, the inundation height in front of the structure will be considerable if the bore has high kinetic energy (high velocity). As shown in Figure 10c, H_{ff} is lower than E_i in all of the cases, indicating that if E_i in front of the seawall can be determined, it is possible to calculate a seawall height that would not be overtopped by a tsunami. Using the definition of the Froude number ($Fr^2 = u^2/gh = V_i^2/gH_i$), and assuming that the energy head of the incoming flow, E_i, will equal the water level at the wall, the ratio between the wall height that is required to completely block a tsunami, h_{w0} and the undisturbed bore height, H_i, could be estimated as:
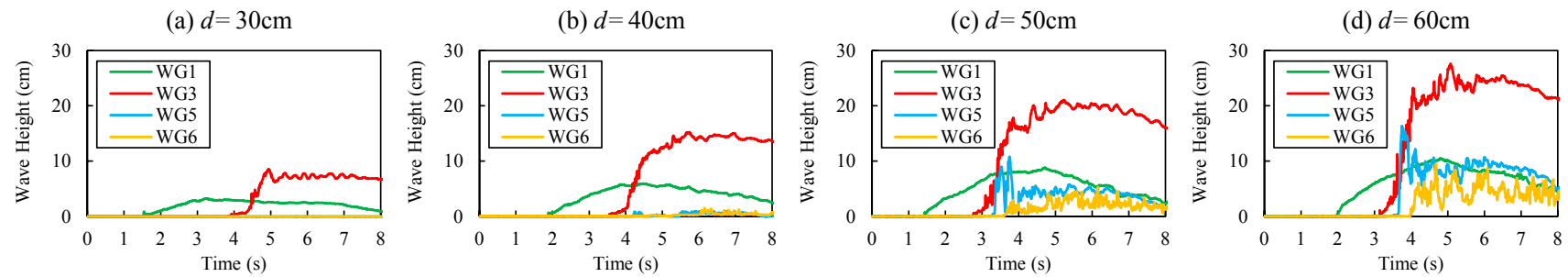
$$h_{w0}/H_i = (Fr^2/2 + 1) \tag{2}$$

Figure 6. Time history of water elevation of representative bores attacking the low vertical wall. All cases shown are for no water in front of the gate (*h* = 0 cm), and depths of water in the tank *d* = 30, 40, 50 and 60 cm (**a–d**). The location of each wave gauge is indicated in Figure 1.
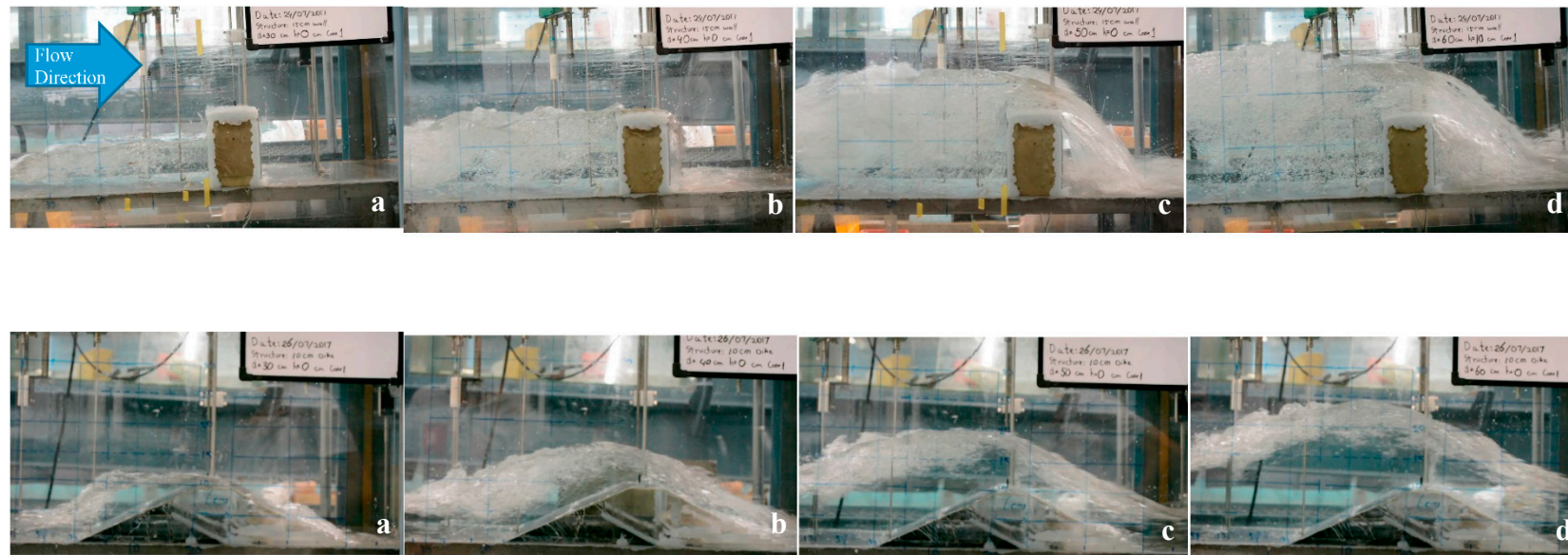

Figure 7. Comparison of different overflowing patterns for various types of incident bores, for the low tsunami wall and dyke structure. All photographs are for the *h* = 0 cm cases, and *d* = 30, 40, 50 and 60 cm (**a–d**). Flow direction is from left to right in all figures.

Figure 8. Comparison of incident and overtopping wave profiles for the three structures studied, for h = 50, d = 0 cm. From left to right: bore approaching the structure (t = 0 s is when the bore reaches WG3), bore hitting the structure, beginning of overtopping, quasi-stationary overtopping flow. For the vertical structure no overtopping was recorded, as the purpose of having this case was to study what effect would an "infinite" wall have on the incident bore.

This seems to give a crude, but safe, estimate for the required wall height. For lower walls (in terms of h_w/E_i), the measured water depths in front of the wall are somewhat lower than for the high wall—up to roughly 20% to 30%—as can be seen in Table 1.

In the present experiments, the authors were interested in the ratio of H_b/H_i, in order to understand the inundation that is caused by a tsunami after overtopping the dyke. In Figure 11, the ratio is summarized in terms of H_i, $V_i^2/2g$ and E_i, respectively. All of the figures show a similar tendency. That is, for the case of low H_i, $V_i^2/2g$, and E_i, the wave did not substantially overtop the structure, and this was capable of completely stopping the wave. As those values increased, the ratio H_b/H_i also increased, indicating that the wave had started to overtop the structure. Eventually, if those values were high enough, the bore bypassed the structure, without suffering any significant influence from the obstruction (with H_b/H_i of almost 90% for the case of the dyke). In order to further clarify the influence of the structure, the authors divided these values by the height of structure (H_w), as shown in Figure 12. Figure 12a,b indicates that inundation after the structure was observed regardless of the horizontal velocity values. This means that even when the tsunami height and velocity head is lower than the structure height ($H_i < H_w$, $V_i^2/2g < H_w$), the tsunami overtopped the structure. In contrast, when the ratio of E_i/H_w is less than 1.0, the ratio of H_b/H_i is almost zero (Figure 12c), meaning that the tsunami did not overtop the structure when the specific energy was lower than the structure height.

The results indicate that the specific energy of incident tsunami is of paramount important when determining whether the bore will overtop the structure or not. In order to know whether inundation will occur or not after the structure it is clear that engineers designing coastal structures should not only consider the incident bore height or velocity, but also its specific energy.
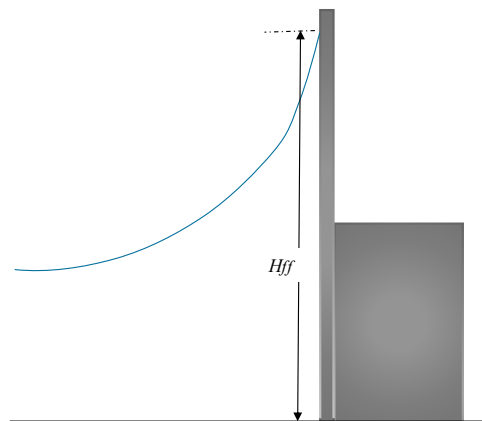

Figure 9. Incident wave parameters. H_{ff} is the maximum values of the surface profile of the wave as it impacts the high seawall, as given by WG4.
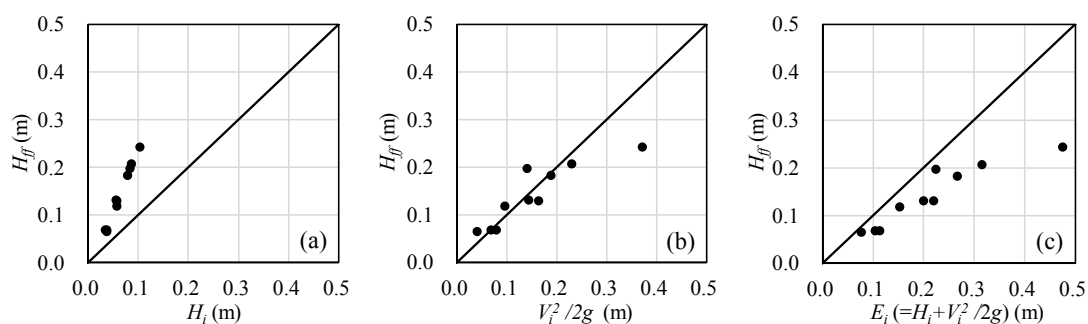

Figure 10. Relationship between the wave depth in front of the high wall (H_{ff}) and (**a**) the incident wave height (H_i), (**b**) velocity head ($V_i^2/2g$), and (**c**) the specific enegy ($H_i + V_i^2/2g$).
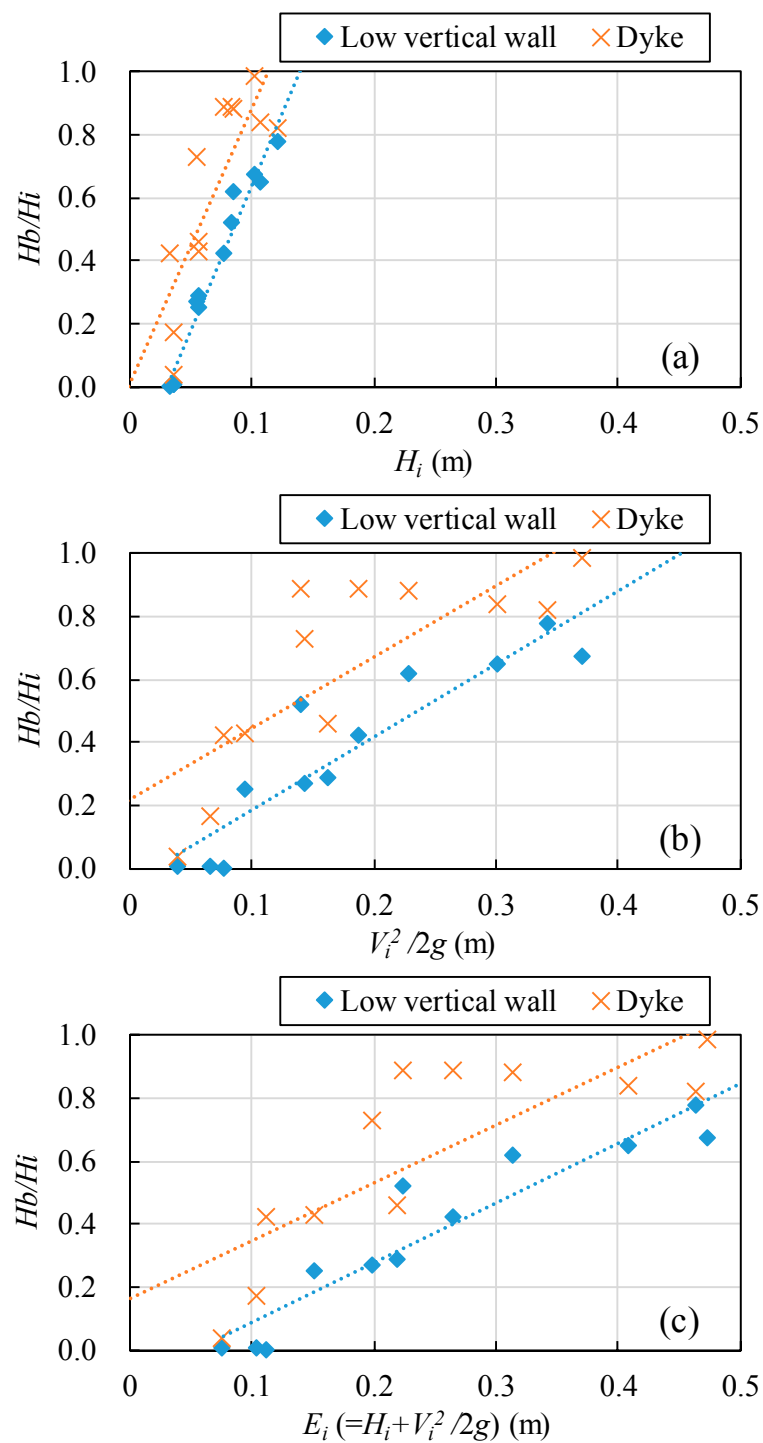
Figure 11. Relationship between the ratio of wave depth after the wall (H_b) and the incident wave height (H_i), and (**a**) the incident wave height (H_i), (**b**) velocity head ($V_i^2/2g$), and (**c**) the specific energy ($H_i + V_i^2/2g$).
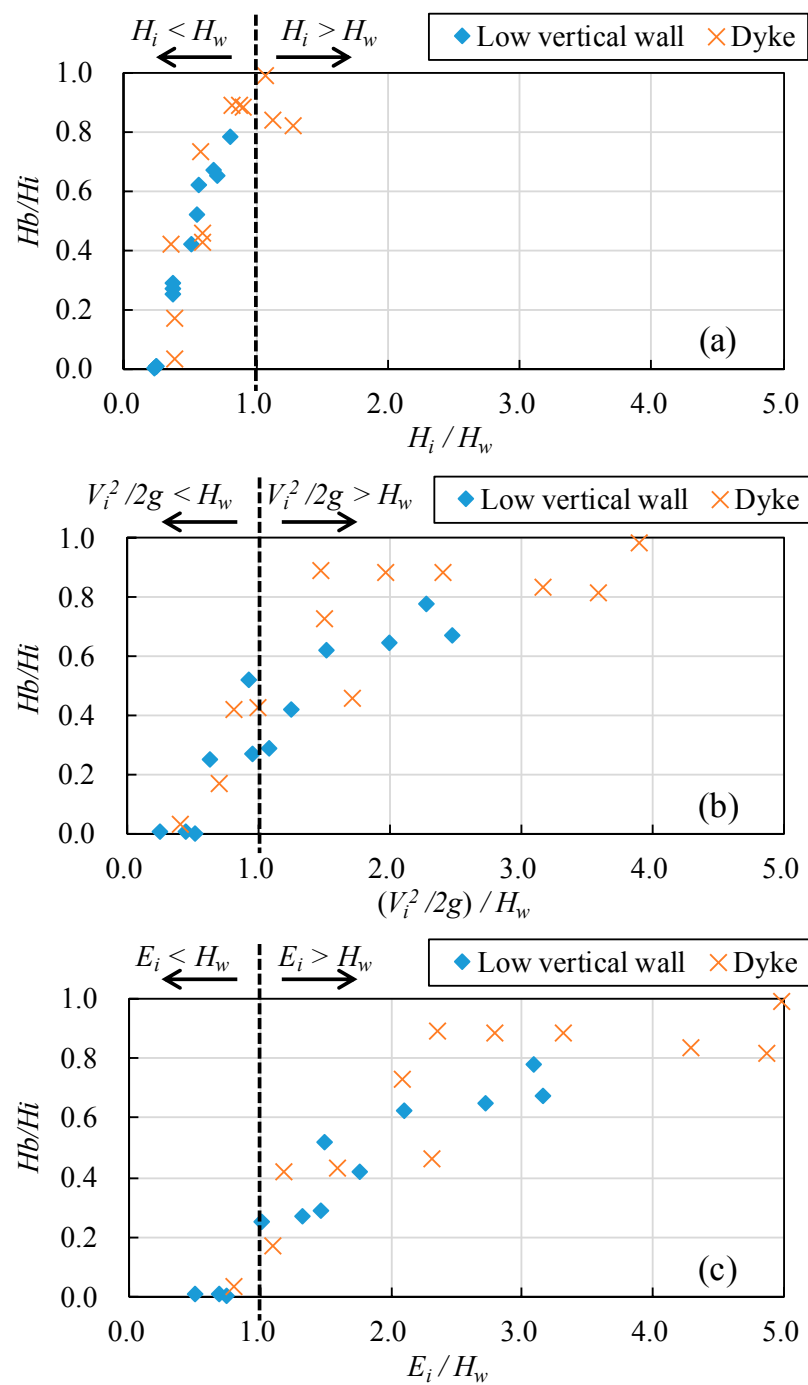
Figure 12. Relationship between the ratio of wave depth after the wall (H_b) and the incident wave height (H_i), and the dimensionless values: (**a**) H_i/H_w; (**b**) $(V_i^2/2g)/H_w$; (**c**) E_i/H_w.

4. Engineering Implications and Discussion

Based on the experimental results, it was possible to provide a rough estimate of the inundation height after a structure of a given height H_w, given the specific energy of the incident bore E_i (which can be calculated according to its incident wave height H_i and the wave velocity V_i), as shown in

Figure 13. In this study, the ratio of H_b/H_i was determined based on the experimental results that are outlined earlier, resulting in the following expression:

$$H_b/H_i = \tanh\left(0.51\frac{E_i}{H_w} - 0.36\right)\left(R^2 = 0.89\right) \tag{3}$$

Note that the wave behaviour is similar for both dyke shapes, according to the data collapse in the figure. Generally speaking, this equation should only be considered as valid for structures and tsunamis where $0.2 < H_i/H_w < 1.3$, and is only applicable for flat beaches and structures with fixed slopes that have not suffered any damage.

The equation can be used for a first approximation of the final answer, and more laboratory experiments, together with computer simulations, are needed to arrive to a more precise equation. The benefit of obtaining such answers obviously lies in facilitating the work of practicing engineers, who in many occasions require rough formulas to arrive at approximate answers that can then be more precisely modelled using inundation and propagation software.
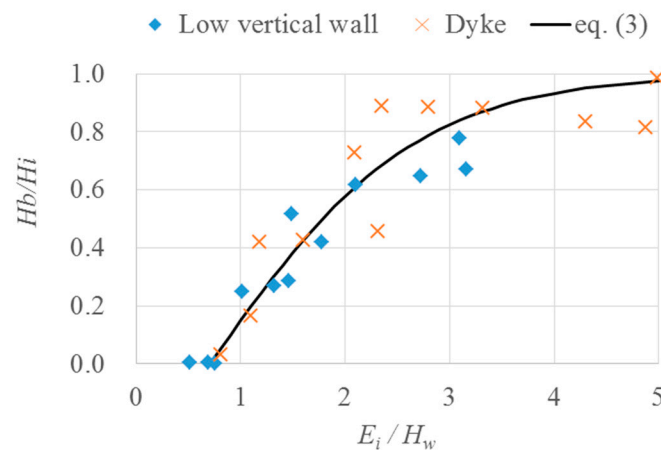

Figure 13. Relationship between the ratio of wave depth after the wall [H_b] to the incident wave height [H_i] and the E_i/H_w.

The results highlight the need to also consider the incident bore velocity in the design of coastal protection structures. The necessity for such an approach was clearly highlighted by video footage of the *2011 Tohoku Earthquake Tsunami*, which showed how in some regions the wave manifested itself as a slow bore or rapidly rising tide, while in others it appeared as a high velocity bore. The difference in wave type has important implications for the design of coastal dykes, as under the present Level 1 and 2 protection philosophy employed in Japan, dykes should protect coastal settlements against the expected inundation that could be brought about as a result of a Level 1 tsunami. Figure 13 shows how this problem is not just as simple as building a dyke of a height equivalent to the incident tsunami height, and that careful consideration should be given to the overtopping wave process.

The actual failure mechanisms of the dyke itself were not considered, as these are outside of the scope of the present work. Nevertheless, it is important to note that following the failure mechanisms described by many researchers [6,8,23], the newly rebuilt coastal structures have been significantly improved, especially regarding leeward protection. This is also an important topic for future research.

5. Conclusions

Laboratory experiments using dam-break bores were conducted on three different types of structures, namely an "infinite" vertical wall, a low vertical wall, and a horizontal dyke, with the aim of understanding how the overtopping processes affects the inundation height behind the structures. The results indicate that the amount of energy in the approaching bore (which is a function of its

height and velocity) is critical in determining whether the structure will be overtopped or not. This fact highlights the need to move away from only considering the inundation height of the tsunami wave at the beach, and also consider its velocity. Given that the current design philosophy in Japan requires dykes to be able to prevent coastal areas from being flooded by a Level 1 tsunami, such considerations are important. Allowing for reduced flooding would be needed to improve the effectiveness of the soft engineering methods [33,36]. Nevertheless, it is important to note that for the case of the *2011 Tohoku Earthquake Tsunami* there is considerable evidence indicating that structures were quite effective at mitigating tsunami damage, and thus the bores might not have had as much energy as some of those that were modelled in the present work. Therefore, it is imperative that the bore propagation process is further clarified, potentially looking at issues of energy dissipation at the "beach" in front of the structures, by increasing the roughness of the materials and analysing the effects of any structures placed at the forefront of the beach.

As conducting detailed inundation simulations considering a variety of structures can be time consuming, the authors attempted to develop an intuitive graphical representation that can easily allow a practicing engineer to calculate the expected inundation behind a dyke of a given size. This is not a substitute for inundation simulations, but can allow for a quick estimation of the parameters involved, which can be useful in preliminary design. It is clear that much more work is needed to arrive at a more precise design methodology. The authors plan to continue this work by analysing a wide range of structures, and conduct computer simulations of the far-field flow and its transformation as it reaches the coastline.

Author Contributions: Miguel Esteban, Toni Glasbergen, Tomoyuki Takabatake, Shinsaku Nishizaki and Yuta Nishida performed the experiments. The analysis was conducted by the five authors mentioned previously, plus Bas Hofland and Ioan Nistor. The experiments were originally designed by the authors mentioned up to this point, plus Jacob Stolle and Tomoya Shibayama. Jeremy Bricker and Hiroshi Takagi provided highly critical input regarding the behavior of tsunami bores as they reached coastal structures, and thoroughly reviewed the documents to ensure scientific accuracy. The document was written by all authors (with the exception of Shinsaku Nishizaki and Yuta Nishida), and underwent four rounds of internal review, with all authors making significant direct input and alterations to the text.

Conflicts of Interest: The authors declare no conflict of interest.

References

1. Mori, N.; Takahashi, T. The 2011 Tohoku Earthquake Tsunami Joint Survey Group (2012). Nationwide post event survey and analysis of the 2011 Tohoku Earthquake Tsunami. *Coast. Eng. J.* **2012**, *54*, 1250001. [CrossRef]

2. Mikami, T.; Shibayama, T.; Esteban, M.; Matsumaru, R. Field survey of the 2011 Tohoku Earthquake and tsunami in Miyagi and Fukushima Prefectures. *Coast. Eng. J.* **2012**, *54*, 1250011. [CrossRef]

3. Ranghieri, F.; Ishiwatari, M. *Learning from Megadisasters: Lessons from the Great East Japan Earthquake*; World Bank Publications: Washington, DC, USA, 2008; Available online: https://openknowledge.worldbank.org/bitstream/handle/10986/18864/9781464801532.pdf?sequence=1 (accessed on 20 November 2017).

4. Shibayama, T.; Esteban, M.; Nistor, I.; Takagi, H.; Danh Thao, N.; Matsumaru, R.; Mikami, T.; Aranguiz, R.; Jayaratne, R.; Ohira, K. Classification of tsunami and evacuation areas. *J. Nat. Hazards* **2013**, *67*, 365–386. [CrossRef]

5. Tomita, T.; Yeom, G.S.; Oyugai, M.; Niwa, T. Breakwater effects on tsunami inundation reduction in the 2011 off the Pacific coast of Tohoku Earthquake. *J. Japan Soc. Civ. Eng. Ser. B2* **2012**, *68*, 156–160. Available online: https://www.jstage.jst.go.jp/article/kaigan/68/2/68_I_156/_article (accessed on 20 November 2017). [CrossRef]

6. Kato, F.; Suwa, Y.; Watanabe, K.; Hatogai, S. Mechanism of coastal dike failure induced by the Great East Japan Earthquake Tsunami. In Proceedings of the 33nd International Conference on Coastal Engineering, Santander, Spain, 1–6 July 2012.

7. Esteban, M.; Jayaratne, R.; Mikami, T.; Morikubo, I.; Shibayama, T.; Danh Thao, N.; Ohira, K.; Ohtani, A.; Mizuno, Y.; Kinoshita, M.; et al. Stability of breakwater armour units against tsunami attack. *J. Waterw. Ports Coast. Ocean Eng.* **2014**, *140*, 188–198. [CrossRef]

8. Jayaratne, M.P.R.; Premaratne, B.; Adewale, A.; Mikami, T.; Matsuba, S.; Shibayama, T.; Esteban, M.; Nistor, I. Failure mechanisms and local scour at coastal structures induced by Tsunami. *Coast. Eng. J.* **2016**, *58*, 1640017. [CrossRef]

9. Goda, Y. *Random Seas and Design of Maritime Structures*; University of Tokyo Press: Tokyo, Japan, 1985; ISBN 4130681109.

10. Tanimoto, K.; Furakawa, K.; Nakamura, H. Hydraulic resistant force and sliding distance model at sliding of a vertical caisson. In Proceedings of the International Conference on Coastal Engineering, Orlando, FL, USA, 2–6 September 1996; pp. 846–850. (In Japanese)

11. Esteban, M.; Takagi, H.; Shibayama, T. Improvement in calculation of resistance force on caisson sliding due to tilting. *Coast. Eng. J.* **2007**, *49*, 417–441. [CrossRef]

12. Tanimoto, L.; Tsuruya, K.; Nakano, S. Tsunami force of Nihonkai-Chubu Earthquake in 1983 and cause of revetment damage. In Proceedings of the 31st Japanese Conference on Coastal Engineering, Tokyo, Japan, 13–14 April 1984.

13. Ikeno, M.; Mori, N.; Tanaka, H. Experimental study on tsunami force and impulsive force by a drifter under breaking bore like Tsunamis. *Coast. Eng. J.* **2001**, *48*, 846–850.

14. Ikeno, M.; Tanaka, H. Experimental study on impulse force of drift body and tsunami running up to land. *Ann. J. Coast. Eng.* **2003**, *50*, 721–725.

15. Mizutani, S.; Imamura, F. Hydraulic experimental study on wave force of a bore acting on a structure. *Coast. Eng. J.* **2000**, *47*, 946–950.

16. Esteban, M.; Danh Thao, N.; Takagi, H.; Shibayama, T. Laboratory experiments on the sliding failure of a caisson breakwater subjected to solitary wave attack. In Proceedings of the Eighth ISOPE Pacific/Asia Offshore Mechanics Symposium, Bangkok, Thailand, 10–14 November 2008.

17. Esteban, M.; Danh Thao, N.; Takagi, H.; Shibayama, T. Pressure exerted by a solitary wave on the rubble mound foundation of an armoured caisson breakwater. In Proceedings of the 19th International Offshore and Polar Engineering Conference, Osaka, Japan, 21–26 June 2009.

18. Esteban, M.; Morikubo, I.; Shibayama, T.; Aranguiz Muñoz, R.; Mikami, T.; Danh Thao, N.; Ohira, K.; Ohtani, A. Stability of rubble mound breakwaters against solitary waves. In Proceedings of the 33nd International Conference on Coastal Engineering, Santander, Spain, 1–6 July 2012.

19. Madsen, P.A.; Furhman, D.R.; Schaffer, H.A. On the solitary wave paradigm for tsunamis. *J. Geophys. Res.* **2008**, *113*, C12012. [CrossRef]

20. Goseberg, N.; Wurpts, A.; Schlurmann, T. Laboratory-scale generation of tsunami and long waves. *Coast. Eng.* **2013**, *79*, 57–74. [CrossRef]

21. Sakakiyama, T. Stability of armour units of rubble mound breakwater against Tsunamis. In Proceedings of the 33rd International Conference on Coastal Engineering, Santander, Spain, 30 June–5 July 2012.

22. Hanzawa, M.; Matsumoto, A.; Tanaka, H. Stability of Wave-dissipating concrete blocks of detached breakwaters against Tsunami. In Proceedings of the 33rd International Conference on Coastal Engineering, Santander, Spain, 1–6 July 2012.

23. Mikami, T.; Matsuba, S.; Shibayama, T. Flow Geometry of Overflowing Tsunamis Around Coastal Dykes. In Proceedings of the Coastal Engineering Proceedings 2014, Seoul, Korea, 15–20 June 2014; Available online: https://journals.tdl.org/icce/index.php/icce/article/view/7615/pdf_839 (accessed on 1 June 2016).

24. Nandasena, N.A.K.; Sasaki, Y.; Tanaka, N. Modelling field observations of the 2011 Great East Japan tsunami: Efficacy of artificial and natural structures on tsunami mitigation. *Coast. Eng.* **2012**, *67*, 1–13. [CrossRef]

25. Stansby, P.; Xu, R.; Rogers, B.D.; Hunt-Raby, A.; Borthwick, A.G.L.; Taylor, P.H. Modelling overtopping of a sea defence by shallow-water Boussinesq, VOF and SPH methods. In *Flood Risk Management: Research and Practice*; Samuels, P., Huntington, S., Allsop, W., Harrop, J., Eds.; CRC Press: Boca Raton, FL, USA, 2008.

26. Hunt-Raby, A.; Borthwick, A.G.L.; Stansby, P.K.; Taylor, P.H. Experimental measurement of focused wave group and solitary wave overtopping. *J. Hydraul. Res.* **2011**, *49*, 450–464. [CrossRef]

27. Chock, G.; Robertson, I.; Kriebel, D.; Nistor, I.; Francis, M.; Cox, D.; Yim, S. *The Tohoku, Japan, Tsunami of March 11, 2011: Effects on Structures*; Special Earthquake Report (2011) Learning from Earthquakes; Earthquake Engineering Research Institute: Oakland, CA, USA, September 2011.

28. Supparsi, A.; Koshimura, S.; Imai, K.; Mas, E.; Gokon, H.; Muhari, A.; Imamura, F. Damage characteristic and field survey of the 2011 Great East Japan Tsunami in Miyagi Prefecture. *Coast. Eng. J.* **2012**, *54*, 1250005.

29. Omira, R.; Baptista, M.A.; Leone, F.; Matias, L.; Mellas, S.; Zourarah, B.; Miranda, J.M.; Carrilho, F.; Cherel, J.P. Performance of coastal sea-defence infrastructure at El Jadida (Marocco) against tsunami threat: Lessons learned from the Japanese 11 March tsunami. *Nat. Hazards Earth Syst. Sci.* **2013**, *13*, 1779–1794. [CrossRef]

30. Latcharote, P.; Suppasri, A.; Hasegawa, N.; Takagi, H.; Imamura, F. Effect of breakwaters on reduction of fatality ratio during the 2011 Great East Japan Earthquake and Tsunami. *J. Jpn. Soc. Civ. Eng. Ser. B2* **2016**, *72*, 1591–1596. [CrossRef]

31. Cyranoski, D. After the deluge: Japan is rebuilding its coastal cities to protect people from the biggest tsunamis. *Nature* **2012**, *483*, 141–143. [CrossRef] [PubMed]

32. Takagi, H.; Bricker, J. Assessment of the effectiveness of general breakwaters in reducing tsunami inundation in Ishinomaki. *Coast. Eng. J.* **2014**, *56*, 21. [CrossRef]

33. Okumura, N.; Jonkman, S.; Esteban, M.; Hofland, B.; Shibayama, T. A method for Tsunami risk assessment—A case study for Kamakura, Japan. *Nat. Hazards* **2017**, *88*, 1451–1472. [CrossRef]

34. San Carlos-Arce, R.; Onuki, M.; Esteban, M.; Shibayama, T. Risk awareness and intended tsunami evacuation behaviour of international tourists in Kamakura City, Japan. *Int. J. Disaster Risk Reduct.* **2017**, *23*, 178–192. [CrossRef]

35. Takabatake, T.; Shibayama, T.; Esteban, M.; Ishii, H.; Hamano, G. Simulated Tsunami evacuation behaviour of local residents and visitors in Kamakura, Japan. *Int. J. Disaster Risk Reduct.* **2017**, *23*, 1–14. [CrossRef]

36. Jonkman, S.N.; Penning-Rowsell, E. Human instability in flood flows. *J. Am. Water Resour. Assoc.* **2008**, *44*, 1208–1218. [CrossRef]

37. Dressler, R.F. Comparison of theories and experiments for hydraulic dam-break wave. *Int. Assoc. Sci. Hydrol.* **1954**, *38*, 319–328.

38. Estrade, J.; Martinot, A. Ecoulment consecutif a la suppression dun barrage dans un canal horizontal de section rectangulaire. *C. R. Hebd. Seances L'Acad. Sci.* **1964**, *259*, 4502. (In French)

39. Chanson, H. Analytical solutions of laminar and turbulent dam break wave. In Proceedings of the International Conference on Fluvial Hydraulics, Lisbon, Portugal, 6–8 September 2006; Ferreira, R.M.L., Alves, E.C.T.L., Leal, J.G.A.B., Cardoso, A.H., Eds.; Taylor & Francis Groupe: London, UK, 2006; Volume 1, pp. 465–474.